Carbon *K* Edge in Graphite Measured Using Electron-Energy-Loss Spectroscopy

Brian M. Kincaid, A. E. Meixner, and P. M. Platzman
Bell Laboratories, Murray Hill, New Jersey 07974
(Received 10 March 1978)

We have measured the carbon *K* edge in graphite using inelastic-electron-scattering spectroscopy. The extended x-ray absorption fine structure is in good agreement with theory for the first-neighbor atoms at a distance of 1.42 Å. The momentum dependence of the edge structure is in qualitative agreement with a simple band-structure picture. A comparison of the signal counting rates for electron-energy-loss and photoabsorption experiments shows that the energy-loss method is competitive with synchrotron radiation sources up to about 1000 eV.

We report the measurement of the *K*-edge photoabsorption spectrum of carbon in graphite using inelastic electron scattering spectroscopy and present a quantitative analysis of the extended x-ray absorption fine structure (EXAFS) modulation for graphite. The high counting rates obtainable using this technique make it possible to measure EXAFS with a good signal-to-noise ratio and to observe the momentum transfer dependence of the absoprtion cross section, which is not possible in an ordinary absorption experiment using photons. The technique permits the measurement of EXAFS and other effects over a large range of energies and is competitive with or superior to present synchrotron radiation methods. We compare the two techniques later in the paper.

When high-energy electrons ($E_i \approx 200$ keV) are scattered from a thin foil of material the energy lost by the scattered electron is a direct measure of the electronic excitation spectrum. The differential cross section for such a weak scattering event is given by Platzman and Wolff[1]:

$$\frac{d^2\sigma}{d\Omega\, d\omega} = \frac{4r_0^2}{(\hbar q/mc)^4} S(q,\omega), \tag{1}$$

where $r_0^2 = e^4/m^2c^4$. Here

$$S(q,\omega) = \sum_{i,f} |\langle f | \sum_j \exp(i\vec{q}\cdot\vec{r}_j) | i\rangle|^2 \delta(\omega_f - \omega_i - \omega). \tag{2}$$

The momentum transfer q, for particles of incident momentum q_i and for nearly elastic collisions is determined by the scattering angle, $q = 2q_i \sin\frac{1}{2}\theta$.

If $|i\rangle$ is a core state with a radius r_c and $qr_c \ll 1$, and if the electrons are independent (Hartree approximation), then

$$S(q,\omega) = q^2 \textstyle\sum_f |\langle f | \hat{\epsilon}_q \cdot \vec{r} | i\rangle|^2 \delta(\omega_f - \omega_i - \omega). \tag{3}$$

Here $\hat{\epsilon}_q$ is a unit vector in the $\vec{q}$ direction. Hence the electron scattering rate in the dipole approximation is proportional to the optical absorption cross section at frequency ω with polarization $\hat{\epsilon}_q$. We will return to a direct comparison of these rates later.

Figure 1 shows electron-energy-loss spectra for thin films of crystalline graphite and amorphous carbon. These curves are raw data with no background removal or smoothing applied. The inset in the upper right of Fig. 1 shows an expanded view of the edge structure for two values of the transverse momentum transfer. The sharp rise near 285 eV is the *K*-shell threshold, and the modulation above the edge is the EXAFS. The second inset in Fig. 1 shows the spectrum of amorphous carbon. The weak EXAFS is due to the disorder in the structure. The spectra were

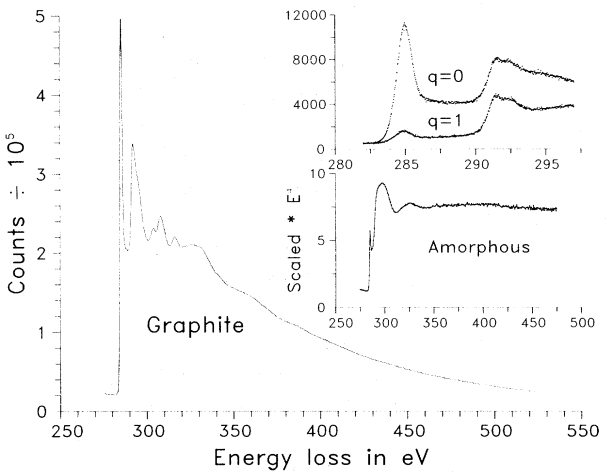

FIG. 1. Energy-loss spectra of crystalline graphite and amorphous carbon. The inset in the upper right shows the momentum-transfer dependence of the near-edge structure for graphite for momentum transfers of 0 and 1 Å^{-1}, scaled so that the edges near 291 eV have the same step height. The second inset shows the spectrum for amorphous carbon, scaled by E^4 to compensate for the decaying signal at higher energies seen in the graphite spectrum. The weak EXAFS is characteristic of an amorphous system.

measured using an inelastic-electron-scattering spectrometer having a beam energy of 200 keV, a beam current of approximately 1 μA,[2] an energy resolution of approximately 0.5 eV, and a transverse momentum resolution of 0.1 Å^{-1} (half-width), with an integration time of 200 sec per point, for a total of about 3 h data collection for the graphite data. The graphite sample was a thin (~500-Å) flake mounted[3] with the c axis parallel to the incident beam. The amorphous carbon sample was a commercial electron microscope substrate.[4] We have tentatively indentified the peak at 285 eV as the transition from the 1s core state to the p_z-like (z along the c axis) π band of graphite.[5] This empty band is pinned at the Fermi surface at the point P (or K) in the Brillouin zone. The edge has a peaked shape with a width of a few eV simply because the band is extremely flat (to within 2 eV) over a good portion of the Brillouin zone. The peak energy of 285 ± 0.5 eV is in good qualitative agreement with the quoted[6] 284 ± 1 eV found in published ESCA (electron spectrosocpy for chemical analysis) measurements of graphite. The edge at 291 eV is to be identified with a transition to a broader σ band which has p_{x-y} symmetry.

The variation in relative intensity of the two transitions is explained by noting that transitions to the π band are driven by the longitudinal component of momentum transfer, q_z, while the σ transitions are coupled to q_{x-y}. In this experiment q_z is essentially constant because there is a minimum momentum transfer $q_{\min}$ corresponding to the loss of roughly 300 eV of electron energy, and, for small scattering angles, $q_{\min}$ is essentially along the z direction, so that we have, for small energy loss ΔE, $q_{\min} \approx q_z \approx m\Delta E/\hbar^2 q_i$. On the other hand, q_{x-y} increases as the scattering angle is increased, and so, as a function of scattering angle or q_{x-y} the π transition should have an approximately $1/q^4$ dependence while the σ-transition should have a $1/q^2$ as is roughly borne out in Fig. 1, where the $q = 1$ Å^{-1} data have been scaled so that the edges at 291 eV have the same step height. This says that information about final-state symmetry can be gained from a study of the q dependence of the edge structure.[7] In the amorphous carbon data there is, as expected, no q dependence of the shape of the edge structure. In addition, over this range of momentum transfer there is essentially no change in the EXAFS in either spectrum.

Figure 2 shows the EXAFS part of the spectrum in Fig. 1. The smooth part of the absorption background has been removed, and the resulting oscillations multiplied by k^2, where k is the photoelectron's wave vector,[8] to compensate partially for the decay of the EXAFS amplitude function.[8] The inset in Fig. 2 shows the magnitude of the Fourier transform of the EXAFS, and shows clearly the peaks due to the first three shells of in-plane neighbors in graphite at distances of 1.42, 2.46, and 2.84 Å. The second two shells are not resolved in the Fourier transform. The distances along the c axis are not seen, because of the large thermal vibration in that direction and also because of the dipole weighting of the EXAFS in the direction $\hat{\epsilon}_q$. The peaks beyond about 5 Å are due to the noise in the data, and, since the noise spectrum is flat, this is a measure of the signal-to-noise ratio for the larger peaks. The dashed curve in the inset is a smooth window function used to extract first-shell EXAFS information.[9] Using theoretical EXAFS phase shifts for carbon,[10] the data in Fig. 2 have been analyzed to determine the nearest-neighbor carbon-carbon distance, resulting in a bond length of 1.42 ± 0.02 Å, in close agreement with the known distance of 1.42 Å. It should be pointed out that EXAFS oscillations can also be observed in other published electron-energy-loss spectra,[11] but, to date, no quantitative analysis has been attempted.

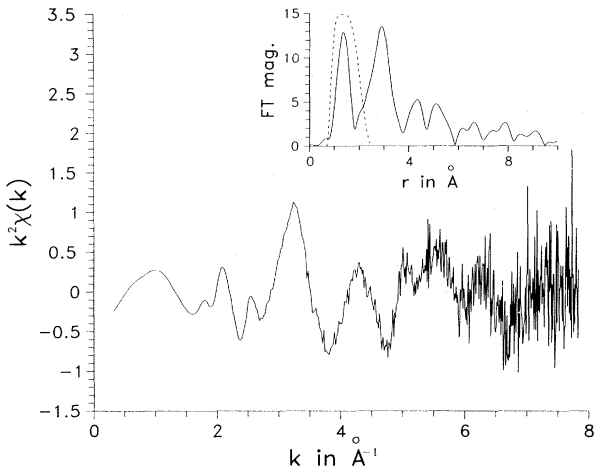

FIG. 2. The EXAFS part of the graphite spectrum in Fig. 1. The smooth background has been removed, energy loss has been changed to k, or photoelectron wave vector, and the oscillatory EXAFS pattern multiplied by k^2. The inset shows the Fourier transform of the data, and shows peaks from the nearest-neighbor atoms. The dashed curve is a filter window isolating the first-shell EXAFS information.

A comparison between electron energy loss and photoabsorption can be made by examining

the counting rates in the two experiments. The cross section in Eq. (1) is simply converted to a counting rate by integrating over the solid-angle acceptance of the electron energy analyzer and multiplying by the incident electron flux (N_e per unit area per second). The counting rate per scatterer then becomes

$$d\Gamma_e = \frac{4\pi r_0^2}{q_i^2(\hbar/mc)^4} N_e \ln\left[1+\left(\frac{q_0}{q_{\min}}\right)^2\right] M(\omega)\, d\omega, \tag{4}$$

where q_0 is the transverse momentum resolution of the electron detector, and

$$M(\omega) = \sum_f |\langle f | \hat{\epsilon}_\beta \cdot \vec{r} | i \rangle|^2 \delta(\omega_f - \omega_i - \omega). \tag{5}$$

For the equivalent photon counting rate,[12]

$$d\Gamma_{\rm ph} = (2\pi)^2 \alpha \omega N_{\rm ph}(\omega) M(\omega)\, d\omega. \tag{6}$$

Here α is the fine-structure constant $e^2/\hbar c$, ω is the photon energy ($\hbar\omega$ is the electron energy loss), and $N_{\rm ph}(\omega)$ is the photon flux per unit bandwidth. The ratio of the two rates for samples of thickness t_e and $t_{\rm ph}$, respectively, is

$$\frac{d\Gamma_e}{d\Gamma_{\rm ph}} = \frac{\alpha}{\pi} \frac{\ln[1+q_0^2/q_{\min}^2]}{(\hbar^2 q_i^2/m^2c^2)\omega} \frac{N_e}{N_{\rm ph}(\omega)} \frac{t_e}{t_{\rm ph}}. \tag{7}$$

In the electron experiment, the sample thickness t_e is determined by multiple inelastic scattering due to plasmons and by the loss of electrons due to elastic scattering at angles larger than the angular acceptance of the electron analyzer. In the photon experiment, optimum signal-to-noise ratio results if the sample has a thickness of $2/\mu$, where μ is the photoabsorption coefficient. Interestingly, near the carbon K-edge energy of 285 eV, t_e and $t_{\rm ph}$ are comparable for graphite (≈ 500 Å), and hence one technique does not have a geat advantage over the other in ease of sample preparation and in data rate for a given sample, other things being assumed equal.

Thus, it can be seen from Eq. (7) that for a given sample thickness, and with the slow energy dependence of the log term in Eq. (7) ignored, the ratio of the electron-energy-loss counts to absorbed photons is roughly proportional to $1/\omega$, and that for an energy loss near the carbon K edge and for the other experimental parameters in the present electron spectrometer, the signal rates for electrons and photons differ by approximately a factor of 10^5. Figure 3 is a comparison of the signal counting rate for electron energy loss from Eq. (7) versus the photon flux available under typical conditions at SPEAR, the Stanford

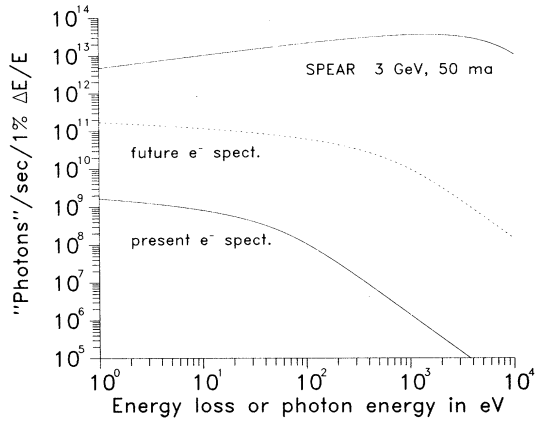

FIG. 3. A comparison of the equivalent "photon flux" for electron energy loss vs synchrotron radiation. See text.

storage ring.[13] The synchrotron radiation photon flux varies as $(\hbar\omega/E_c)^{2/3}$ for $\hbar\omega < E_c$, and as $\exp(-\hbar\omega/E_c)(\hbar\omega/E_c)^{-3/2}$ for $\hbar\omega > E_c$, E_c being the critical energy.[14] The photon flux for SPEAR operating at 3 GeV and 50 mA and for a detector accepting 1 mrad of horizontal angle is shown in the upper solid curve and the bottom solid line is a plot of Eq. (7) for the present electron spectrometer parameters for unit photon flux, i.e., a plot of the equivalent "photon flux" for the electron experiment. Presently available uv monochromators at SPEAR have a net transmission of only about 10^{-5},[15] so that even with the present parameters the signal rate near the carbon K edge (285 eV) is comparable for the two methods. Improvements in the electron-energy-loss method involving higher beam current, parallel detection of energy-loss events rather than the present serial method, and increased angular acceptance in the electron detection system are expected to yield a factor of at least 10^5 improvement in signal rate for the electron technique. The dashed line in Fig. 3 shows Eq. (7) evaluated for such an improved machine, omitting the parallel detection advantage, which could amount to about two orders of magnitude, and which, in principle, could also be gained using synchrotron radiation, even though there are no practical methods for doing this at present. On the other hand, the improvement of present electron-energy-loss techniques is fairly straightforward, and hence opens up the prospect of measuring electronic and structural properties of dilute impurities, surface monolayers, and interfaces in a short time, as well as EXAFS for K edges of the first-row elements and L, M, and N edges of other ele-

ments, all with synchrotron-radiation-like intensities but in a small lab-sized electron-energy-loss machine.

We would like to thank M. Schlüter for several informative discussions on the graphite band structure. We would also like to acknowledge conversations with P. Gibbons and H. Launois, as well as with C. Herring.

[1]P. M. Platzman and P. A. Wolff, *Waves and Interactions in Solid State Plasmas* (Academic, New York, 1973).

[2]G. S. Brown and A. E. Meixner, to be published.

[3]Graphite sample kindly prepared from monochromator-grade pyrolytic graphite by J. Wilson, Bell Laboratories, Murray Hill, N. J.

[4]200-Å film from The Arizona Carbon Foil Co., Tuscon, Ariz.

[5]D. L. Greenway, G. Harber, F. Bussani, and E. Tosatti, Phys. Rev. 178, 1340 (1969).

[6]S. Hagstrom and S. E. Karlsson, Ark. Fys. 26, 451 (1964).

[7]S. G. Slusky *et al.*, Phys. Rev. Lett. 36, 326 (1976); C. H. Chen and J. Silcox, Phys. Rev. B 16, 4246 (1977).

[8]P. A. Lee and G. Beni, Phys. Rev. B 15, 2862 (1977).

[9]P. H. Citrin, P. Eisenberger, and B. M. Kincaid, Phys. Rev. Lett. 36, 1346 (1976); B. M. Kincaid, P. H. Citrin, and P. Eisenberger, to be published.

[10]Carbon phase shift kindly supplied by P. A. Lee.

[11]C. Colliex and B. Jouffrey, Philos. Mag. 25, 491 (1972); J. J. Ritsko *et al.*, Phys. Rev. Lett. 37, 1068 (1976).

[12]R. P. Feynman, *Quantum Electrodynamics* (Benjamin, New York, 1962).

[13]Synchrotron Radiation Research, Stanford Synchrotron Radiation Project Report No. SSRP 76/100, August 1976 (unpublished).

[14]R. A. Mack, Cambridge Electron Accelerator Report No. CEAL-1027, February 1966 (unpublished).

[15]G. S. Brown, private communication.

Concentration-Dependent Collapse of a Large Polymer

J. Naghizadeh and A. R. Massih
Institute of Biochemistry and Biophysics, Tehran University, Tehran, Iran
(Received 3 October 1977)

The observed condensation of DNA in salt solution in the presence of a second polymer of lower molecular weight is treated by straightforward statistical mechanics. We neglect the details of DNA structure and represent it by a simple polymer of large molecular weight interacting via single-contact repulsive forces with a large number of smaller polymers. In this approximation, the derivative of free energy with respect to the size of the large polymer shows a singularity at a critical concentration of smaller polymers.

In recent years a large body of experimental work has accumulated on the collapse of DNA in water-salt solutions in the presence of a second polymer of lower molecular weight. This phenomenon, called Ψ condensation, has been reviewed by Lerman,[1] and it has significant biological relevance since DNA of bacteriophage *T4* at certain concentrations of internal proteins can collapse in a similar manner.[2]

In a typical experiment, DNA of a virus with molecular weight of about 10^8 is dissolved in a salt-water solution of approximately 0.5 molar salt and 10^{-12} molar DNA. If now one adds to this solution a second polymer [typically polyethylene oxide (PEO)] of a molecular weight of about 7000, the hydrodynamic properties of the system DNA–salt-water–PEO undergo drastic change (transition) at a critical concentration of PEO, in this case about 0.3 molar. The change in the hydrodynamic properties such as viscosity or sedimentation coefficient indicate a drastic and sudden change in the mean volume occupied by DNA molecules.[3,4] Spectroscopic and x-ray data also support this interpretation.[5,6] Thus experiments point to the interpretation that a concentration-dependent collapse of DNA (large polymer) is brought about as a result of dissolution of the second polymer of lower molecular weight at a critical concentration of the latter. The process is reversible and has the nature of a phase transition.

Lerman has attempted to explain this phenomenon by simple thermodynamic arguments and has concluded that dominant forces causing the collapse are repulsive forces operating between the large and small polymers. The transition is relatively sharp in DNA solutions because of its considerable size, but polymer fractionation experiments in which a polydisperse polymer solution progressively precipitates in fractions of decreasing molecular weight must be related to this phenomenon.

